NIM

ENERGY AND ANGULAR DISTRIBUTIONS OF ELECTRONS EMITTED AND IONS RECOILED IN PROTON-IMPACT IONIZATION OF HELIUM ATOMS

H. FUKUDA,*

RIKEN, Wako, Saitama 351-01, Japan,

T. WATANABE,

Department of Physics, International Christian University,

Oosawa, Mitaka-shi, Tokyo 181, Japan,

I. SHIMAMURA and L. VÉGH,†

RIKEN Wako, Saitama 351-01, Japan

*Special Researcher, Basic Science Program, RIKEN.

†On leave from: ATOMKI, H-4001, Debrecen, Pf. 51, Hungary.

Abstract

Single ionization of helium atoms in collisions with high-energy protons is theoretically treated in the eikonal distorted-wave approximation. The momentum and angular distributions of the ejected electrons and the recoil ions are calculated as functions of the proton scattering angle.

1 Introduction

Until recently, most measurements on ion-impact ionization had been of the cross sections for single ionization integrated over the projectile scattering angles [1] and of the energy and angular distributions of the ejected electrons [2]. However, recent developments include the measurements of the angular distributions of scattered protons in single and double ionization of helium atoms [3 − 5], and measurements of the proton scattering angle in coincidence with recoil He^+ ions [6] or with emitted electrons [7]. Although such measurements are still limited, much further information may be available in the near future. Therefore it would be worthwhile at this time to study theoretically in detail the energy and angular distributions of the emitted electrons and of the recoil ions for various fixed projectile scattering angles. The aim of this paper is to report the results of such work on single ionization in proton-helium collisions. An approximation referred to as the eikonal distorted-wave approximation is applied. The details of the theory are found elsewhere [8].

In Sec.2 of this paper, only a brief account of the theory is made. The momentum and angular distributions are reported in Sec.3 for electrons and in Sec.4 for recoil ions, and conclusive remarks are made in Sec.5.

2 Eikonal distorted-wave approximation

The scattering angle Θ of protons (with a mass m_p) for distant proton-helium collisions at high energies is determined mainly by the perturbation by the electrostatic potential of the helium atom. For intermediate-distance collisions, Θ is determined mainly by binary collisions with electrons (with a mass m_e). The maximum angle of proton scattering by a stationary, free electron is m_e/m_p or 0.545 mrad. The proton angular distributions measured by Kamber et al. [4 , 5] for collision energies of 3−9 MeV clearly show a shoulder at about 0.55 mrad. This has been explained to be a result of binary proton-electron collisions, which occur for $\Theta < 0.545$ mrad and not beyond [4 , 5]. The angular distributions calculated in the plane-wave Born approximation are in good agreement with the measured angular distributions up to angles slightly larger than 0.545 mrad, and reproduce the binary-collision shoulder [4 , 5].

Scattering of protons by angles beyond the shoulder is determined mainly by close collisions, and is influenced strongly by the Coulomb interaction with the target nucleus, or the α particle. For this reason the proton angular distributions at large angles are not reproducible in the plane-wave Born approximation. The first-order Born method of Ref.[9] reproduces well the angular distribution over a wide angular range at 1 MeV, because it includes approximately the Coulomb interaction between the proton and the helium nucleus. The shoulder is missing at 3 MeV in Ref.[9] because of the neglect of electrons ejected with high energies. This neglect is due to the slow convergence of the partial-wave expansion, employed in Ref.[9], of the wave functions of high-energy ejected electrons.

In the eikonal distorted-wave method of this paper and of Ref.[8], we take into account the distortion of the proton motion from the plane wave by the electrostatic potential $U(R)$ due to the helium atom in the ground state; R is the internuclear distance. We avoid the partial-wave expansion of the wave function of the outgoing electron. This method may be derived as follows [8]. We use atomic units in the expressions in the text.

First, we apply the distorted-wave Born approximation using the distortion potential $U(R)$. In other words, the plane waves for the relative proton-helium motion in the initial and final channels in the expression for the T matrix in the plane-wave Born approximation are replaced by the wave functions distorted by $U(R)$. Normally, the distortion potential must be subtracted from the perturbation potential to be sandwiched between the initial- and final-channel distorted waves. In the present case, however, the distortion potential depends only on the internuclear distance R, and contributes nothing to the T matrix because of the orthogonality of the initial ground state φ_i and the final continuum state φ_f of the helium atom.

Next, the distorted waves are calculated in the eikonal approximation, i.e., are expressed as the product of the plane wave and a factor $\exp(i\gamma)$. In the calculations of the eikonal phase γ, the momentum K_f of the relative motion in the final channel is assumed to be unchanged from that K_i in the initial channel, which is a good approximation at high energies. We refer to this whole procedure as the eikonal distorted-wave method.

The wave function φ_i is described in this work as

$$\varphi_i(\mathbf{r}_1, \mathbf{r}_2) = u_0(\mathbf{r}_1)u_0(\mathbf{r}_2), \tag{1}$$

where the approximate 1s orbital $u_0(\mathbf{r})$ is defined by

$$u_0(\mathbf{r}) = \sqrt{\frac{\zeta^3}{\pi}} \exp(-\zeta r) \tag{2}$$

with the variationally determined value 27/16 of the exponent ζ. The singlet continuum state φ_f is represented by a symmetrized product form

$$\varphi_f(\mathbf{r}_1, \mathbf{r}_2) = \frac{1}{\sqrt{2}} \left[u_c(\mathbf{r}_1)\varphi_+(\mathbf{r}_2) + u_c(\mathbf{r}_2)\varphi_+(\mathbf{r}_1)\right]. \tag{3}$$

Here, $\varphi_+(\mathbf{r})$ is the wave function of the He^+ ion in the ground state, and $u_c(\mathbf{r})$ is a continuum orbital Schmidt-orthogonalized to the orbital $u_0(\mathbf{r})$ as

$$u_c(\mathbf{r}) = u_\kappa^{(-)}(\mathbf{r}) - < u_0, u_\kappa^{(-)} > u_0(\mathbf{r}) \tag{4}$$

with

$$u_\kappa^{(-)}(\mathbf{r}) = (2\pi)^{-3/2}\Gamma(1 - i\eta_\kappa) \exp(-\pi\eta_\kappa/2) \exp(i\underset{\sim}{\kappa} \cdot \mathbf{r}) F(i\eta_\kappa, 1, -i[\kappa r + \underset{\sim}{\kappa} \cdot \mathbf{r}]). \tag{5}$$

The functions Γ and F here are the gamma function and the confluent hypergeometric function as usual, $\underset{\sim}{\kappa}$ is the momentum of the ejected electron, $\kappa = |\underset{\sim}{\kappa}|$, and $\eta_\kappa = -\kappa^{-1}$. The dependence of the cross sections on the quality of the wave functions is discussed in Ref.[8]. The above choice of the wave functions was found to be accurate enough for the present purpose, except for small proton scattering angles Θ less than about 0.1 mrad.

The T matrix in the eikonal distorted-wave approximation, denoted by $T_{fi}^{\rm EDW}(\mathbf{K})$, is expressible in terms of that in the plane-wave Born approximation, denoted by $T_{fi}^{\rm B}(\mathbf{K})$ and analytically calculable, where $\mathbf{K}$ is the momentum transferred from the relative motion to the helium atom in the collision. The resultant expression is [8]

$$T_{fi}^{\rm EDW}(\mathbf{K}) = T_{fi}^{\rm B}(\mathbf{K}) + \int_0^\infty dQ_\perp Q_\perp A(Q_\perp) \int_0^{2\pi} d\phi_Q T_{fi}^{\rm B}(\mathbf{K}+\mathbf{Q}_\perp), \qquad (6)$$

where

$$A(Q_\perp) = \frac{1}{2\pi}\int_0^\infty b\,db\,J_0(Q_\perp b)(\exp[i\gamma(b)]-1), \qquad (7)$$

$$\gamma(b) = -\frac{4\mu}{K_i}[K_0(2\zeta b) + \zeta b K_1(2\zeta b)], \qquad (8)$$

J_0 is the Bessel function of order zero, K_0 and K_1 are modified Bessel functions, μ is the reduced mass of the relative proton-helium motion, $\mathbf{Q} = (\mathbf{Q}_\perp, Z_Q) = (Q_\perp, \phi_Q, Z_Q)$ in the cylindrical coordinates with the Z_Q axis chosen along the momentum $\mathbf{K}_i$ of the relative motion in the initial channel, and $T_{fi}^{\rm B}(\mathbf{K}+\mathbf{Q}_\perp)$ is the value of $T_{fi}^{\rm B}(\mathbf{K}+\mathbf{Q})$ for $Z_Q = 0$. As is seen from these expressions, there is no need of partial-wave expansion of any kind.

The angular distributions of the protons calculated at proton energies E_0 of 300 keV, 500 keV, 1 MeV, and 3 MeV using this method are discussed in Ref.[8]. They agree quite well with the measured angular distributions in the angular region from 0.1 mrad to about 2 mrad, over which the differential cross section ranges over four orders of magnitude. We found a substantial improvement over the plane-wave

Born approximation, especially beyond the binary-collision shoulder, and even over the method of Salin [9]. These encouraging results prompted us to proceed to the study of more detailed information on all the outgoing particles in the ionization process. A part of such work is reported in Ref.[8].

3 Momentum and angular distributions of ejected electrons

The differential cross section calculated directly from the scattering amplitude $T_{fi}^{\rm EDW}(\mathbf{K})$ is quintuply differential in $\hat{\mathbf{K}}$ and the momentum $\underset{\sim}{\kappa}$ of the ejected electron. It may be transformed into the cross section $q(\Theta, \Phi, \kappa_x, \kappa_y, \kappa_z)$ quintuply differential in the proton scattering angles (Θ, Φ) in the laboratory frame of reference, and in $\underset{\sim}{\kappa}$. For visual representation of the angular distributions of the ejected electrons for different fixed values of Θ, a convenient way is to choose the scattering plane $\Phi = 0$, and plot $q(\Theta, 0, \kappa_x, 0, \kappa_z)$ on the κ_x-κ_z plane. Examples of such a plot are shown in Figs.1a–1e for $E_0 = 500$ keV and for $\Theta = 0.1$, 0.4, 0.6, 0.8, and 1.0 mrad.

Integration of the differential cross section $q(\Theta, \Phi, \kappa_x, \kappa_y, \kappa_z)$ over the angles $\hat{\underset{\sim}{\kappa}}$ leads to the cross section doubly differential in κ and Θ, the dependence on Φ vanishing because of the symmetry of the collision system. Figure 2, taken from Ref.[8], shows normalized doubly differential cross sections for $E_0 = 500$ keV as functions of κ, with Θ given as a parameter. Inspection of Figs.1 and 2 for increasing values of Θ provides an understanding of how the momentum of the ejected electrons change with the scattering angle or with the impact parameter of the collision.

For $\Theta = 0.1$ mrad, the single-peak momentum distribution in Fig.2 in the eikonal distorted-wave approximation is reproduced well in the plane-wave Born approximation. In Fig.1a, this peak is seen around the point $(\kappa_x, \kappa_z) = (0,0)$. The peak decays rapidly as either κ in Fig.2 or $(\kappa_x^2 + \kappa_z^2)^{1/2}$ in Fig.1a increases. The electrons are emitted mainly in the x direction in Fig.1a, i.e., perpendicular to the direction of the incidence of the protons, although the emission angle is slightly tilted towards the direction of incidence.

For $\Theta = 0.4$ mrad (Fig.1b), the main peak is shifted to be centered at $(\kappa_x, \kappa_z) \simeq$ (−3,1) a.u. This peak is mainly due to the effect of the binary proton-electron collisions; thus the binary collision effect is already seen at this scattering angle. This peak is reproducible in the plane-wave Born approximation, but another, smaller peak at (0,0) is not.

For $\Theta = 0.6$ mrad, i.e., just above the maximum deflection angle 0.545 mrad in binary proton-electron collisions and where the effects of the binary collisions are still observed quantum mechanically, the κ distribution of Fig.2 in the eikonal distorted-wave approximation has two peaks. The lower-κ peak is unreproducible in the plane-wave Born approximation, but the higher-κ peak is reproducible, is due to the binary collisions [8], and have two additional shoulders. In fact, the higher-κ peak is triple-peaked at higher collision energies. Figure 1c shows that the binary-collision peak has contours that are elongated towards the direction of the proton incidence, the tendency already seen in the binary peak for $\Theta = 0.4$ mrad.

As Θ increases from 0.6 mrad, naturally, the binary peak rapidly decreases and eventually only one peak around $(\kappa_x, \kappa_z) = (0, 0)$ remains, which is unseen in the plane-wave Born approximation.

4 Momentum and angular distributions of recoil ions

In the light of the recent coincidence measurements of the scattered protons and the recoil He^+ ions [6], it would be interesting to transform the cross section $q(\Theta, \Phi, \kappa_x, \kappa_y, \kappa_z)$ into that differential in Θ, Φ, and the momentum $\mathbf{p}_R = (p_{Rx}, p_{Ry}, p_{Rz})$ of the recoil ion, which is denoted here as $\tilde{q}(\Theta, \Phi, p_{Rx}, p_{Ry}, p_{Rz})$. Figures 3a–3c show contour maps of the recoil momentum distribution $\tilde{q}(\Theta, 0, p_{Rx}, 0, p_{Rz})$ on the scattering plane $\Phi = 0$ for $E_0 = 500$ keV, corresponding to Figs.1a–1e.

Let $\mathbf{p}_0$ and $\mathbf{p}_P$ denote the initial and final momenta of the proton. Also, the usual notation is used for their absolute values and their x, y, and z components. Then, the energy and momentum conservation laws lead to an approximate relation between $\underset{\sim}{\kappa}$ and $\mathbf{p}_R$

$$\frac{p_{Rx} + \kappa_x}{p_0} \simeq -\Theta, \tag{9}$$

$$\frac{p_{Rz} + \kappa_z}{p_0} \simeq \frac{p_0 - p_P}{p_0} \simeq \frac{\Delta E}{2E_0}, \tag{10}$$

where ΔE is the energy of transition from the ground to the continuum state of the helium atom, or the sum of the ionization potential (I.P.) and the energy of the emitted electron.

Equations (9) and (10) suggest that the peak around the point $(\kappa_x, \kappa_z) = (0, 0)$ in each of Figs.1a–1e is mapped onto the p_{Rx}-p_{Rz} plane around the point defined by these equations with κ_x and κ_z neglected. Each of Figs.3a–3c indeed contains a peak at this position. The binary peak for $\Theta = 0.6$ mrad in Fig.1c and Fig.2 is mapped according to the full equations (9) and (10) retaining κ_x and κ_z. Because of the upper-left boundary, however, it is unclear in Fig.3b whether there is a peak at this position. Each of Figs.3a–3c has a boundary that indicates that the region outside the boundary is forbidden. In fact, the differential cross section diverges towards the boundary because of the divergence of the Jacobian used in transforming $q(\Theta, \Phi, \kappa_x, \kappa_y, \kappa_z)$ into $\tilde{q}(\Theta, \Phi, p_{Rx}, p_{Ry}, p_{Rz})$. The Jacobian takes a form

$$\left|\frac{D(\underset{\sim}{\kappa})}{D(\mathbf{p}_R)}\right| = \left|1 \pm \frac{m_p \underset{\sim}{\kappa} \cdot \mathbf{p}_P}{p_P\sqrt{F}}\right|, \tag{11}$$

where

$$F = [\mathbf{p}_P \cdot (\mathbf{p}_0 - \mathbf{p}_R)]^2/p_P^2 - (\mathbf{p}_0 - \mathbf{p}_R)^2 - p_R^2/m_\alpha + p_0^2/m_p - 2(\text{I.P.}). \tag{12}$$

Here, m_α is the mass of the alpha particle.

5 Conclusion

Results of the eikonal distorted-wave calculations of single ionization in proton-helium collisions have been presented in the form of contour maps of the differential cross sections $q(\Theta, \Phi, \kappa_x, \kappa_y, \kappa_z)$ and $\tilde{q}(\Theta, \Phi, p_{Rx}, p_{Ry}, p_{Rz})$ on the scattering plane $\Phi = 0$. Judging from the recent developments, briefly mentioned in Sec.1, in coincidence measurements of scattered protons and either ejected electrons or recoil ions, experiments on these differential cross sections may be feasible in the near future for comparison with the present results. The present calculations neglect the effect of charge transfer to continuum, which is important in forward scattering. For detailed information on the energy and angular distributions of emitted electrons and recoil ions for Θ much smaller than the values treated in this paper, calculations including this effect are necessary.

References

[1] For the total proton-impact ionization cross sections, see, for example, M. E. Rudd, Y.-K. Kim, D. H. Madison, and J. W. Gallagher, Rev. Mod. Phys. **57** (1985) 965. M. B. Shah and H. B. Gilbody, J. Phys. B: At. Mol. Phys. **18** (1985) 899.

[2] For example, M. E. Rudd, L. H. Toburen, and N. Stolterfoht, At. Data Nucl. Data Tables **18** (1976) 413; *ibid.* **23** (1979) 405. L. H. Toburen, S. T. Manson, and Y.-K. Kim, Phys. Rev. A**17** (1978) 148.

[3] J. P. Giese and E. Horsdal, Phys. Rev. Lett. **60** (1988) 2018.

[4] E. Y. Kamber, C. L. Cocke, S. Cheng, and S. L. Varghese, Phys. Rev. Lett. **60** (1988) 2026.

[5] E. Y. Kamber, C. L. Cocke, S. Cheng, J. H. McGuire, and S. L. Varghese, J. Phys. B: At. Mol. Opt. Phys. **21** (1988) L455.

[6] R. Dörner, J. Ullrich, H. Schmidt-Böcking, and R. E. Olson, Phys. Rev. Lett. **63** (1989) 147.

[7] G. Schiwietz, Phys. Rev. A**37** (1988) 370.

[8] H. Fukuda, I. Shimamura, L. Végh, and T. Watanabe, Phys. Rev. A, submitted.

[9] A. Salin, J. Phys. B: At. Mol. Opt. Phys. **22** (1989) 3901.

FIGURE CAPTIONS

Fig.1. Contour map of the calculated (κ_x, κ_z) distribution of the electrons emitted in the scattering plane $\Phi = 0$ in single ionization of helium by 500-keV protons. The numbers on the contours represent the differential cross section $q(\Theta, 0, \kappa_x, 0, \kappa_z)$ in atomic units per steradian, and the contours are drawn at intervals of a factor of $10^{1/n}$, n being 2, 3, or 4 depending on the figure. (a) $\Theta = 0.1$ mrad. (b) $\Theta = 0.4$ mrad. (c) $\Theta = 0.6$ mrad. (d) $\Theta = 0.8$ mrad. (e) $\Theta = 1.0$ mrad.

Fig.2. Momentum distribution of the electrons ejected in single ionization of helium by 500-keV protons that are scattered by angles Θ indicated as parameters on the curves. EDW: results of the eikonal distorted-wave approximation normalized by the cross section at Θ integrated over κ. Born: results of the plane-wave Born approximation with the same normalization as EDW. (The Born results for $\Theta = 1.0$ mrad are multiplied by 5.)

Fig.3. Contour map of the calculated (p_{Rx}, p_{Rz}) distribution of the He^+ ions recoiled in the scattering plane $\Phi = 0$ in single ionization of helium by 500-keV protons. The numbers on the contours represent the differential cross section $\tilde{q}(\Theta, 0, p_{Rx}, 0, p_{Rz})$ in atomic units per steradian, and the contours are drawn at intervals of a factor of $10^{1/2}$ in (a) and (b) and $10^{1/4}$ in (c). p_0 is the momentum of the incident protons. (a) $\Theta = 0.1$ mrad. (b) $\Theta = 0.6$ mrad. (c) $\Theta = 1.0$ mrad.

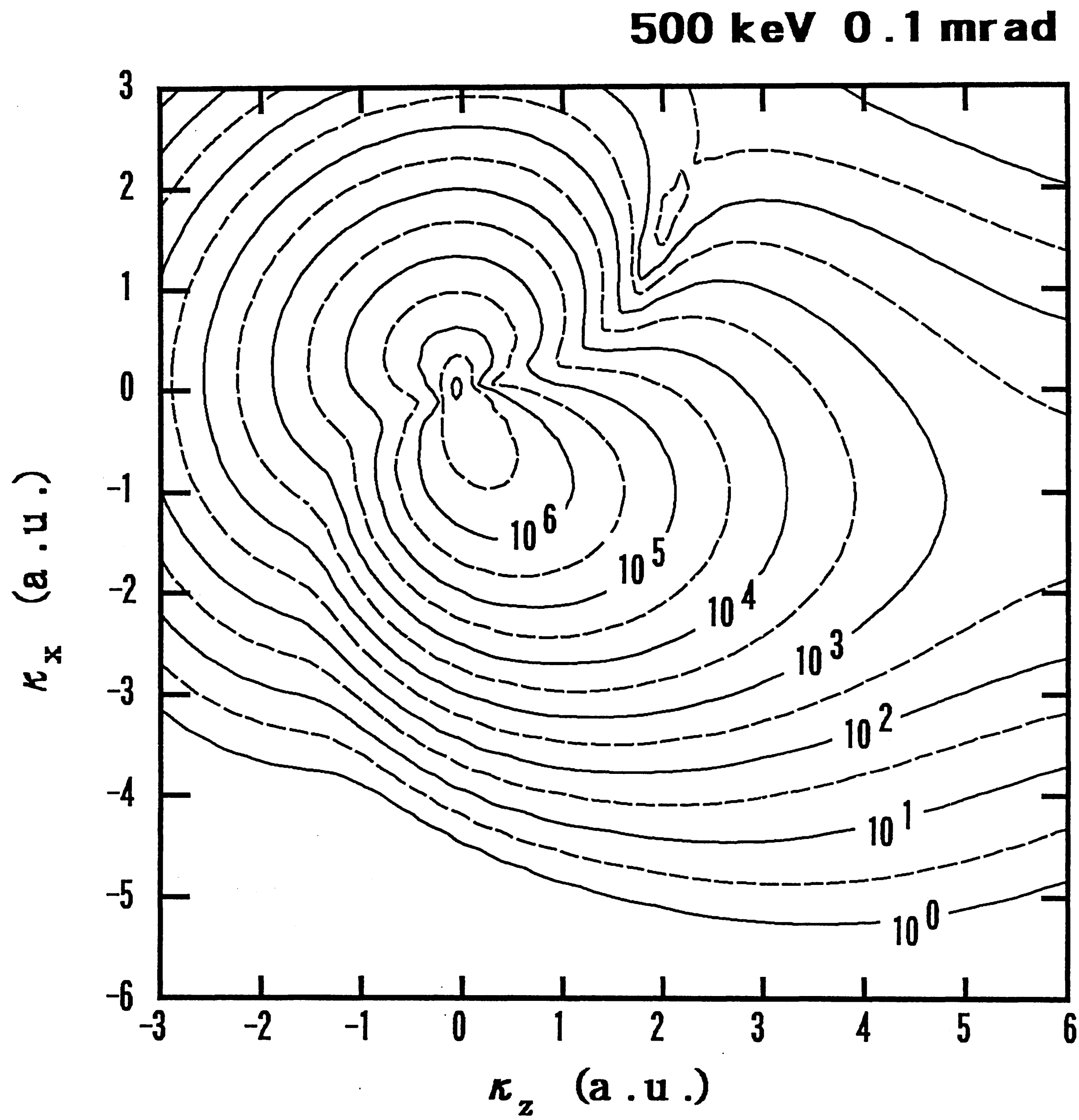

500 keV 0.1 mrad
3
2
1
0
-1
-2
-3
-4
-5
-6
κx (a.u.)
10 6
10 5
10 4
10 3
10 2
10 1
10 0
-3
-2
-1
0
1
2
3
4
5
6
κz (a.u.)

Fig. 1(a)

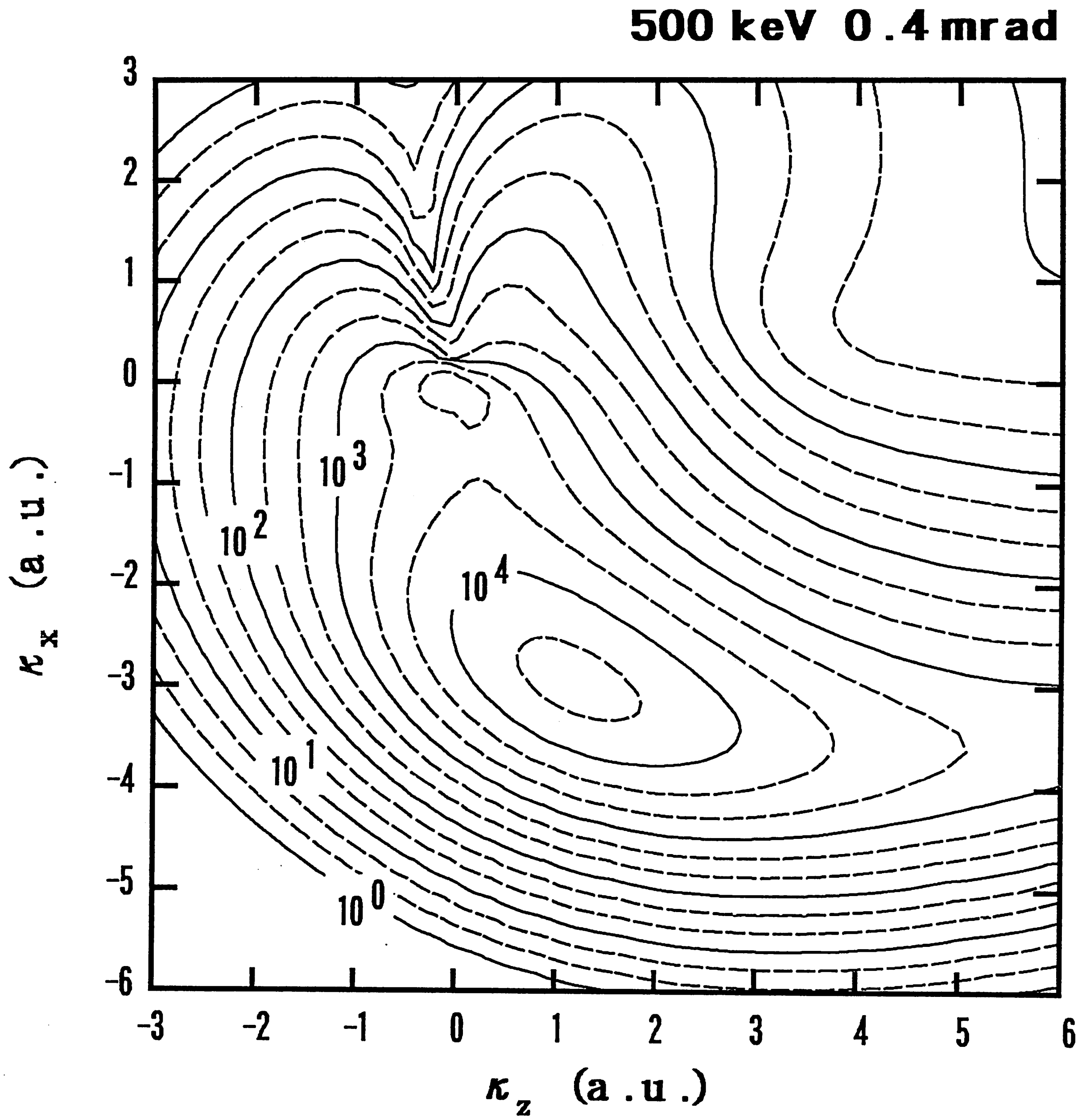
500 keV 0.4 mrad
3
2
1
0
-1
-2
-3
-4
-5
-6
κ_x (a.u.)
10 3
10 2
10 4
10 1
10 0
-3
-2
-1
0
1
2
3
4
5
6
κ_z (a.u.)

Fig. 1(b)

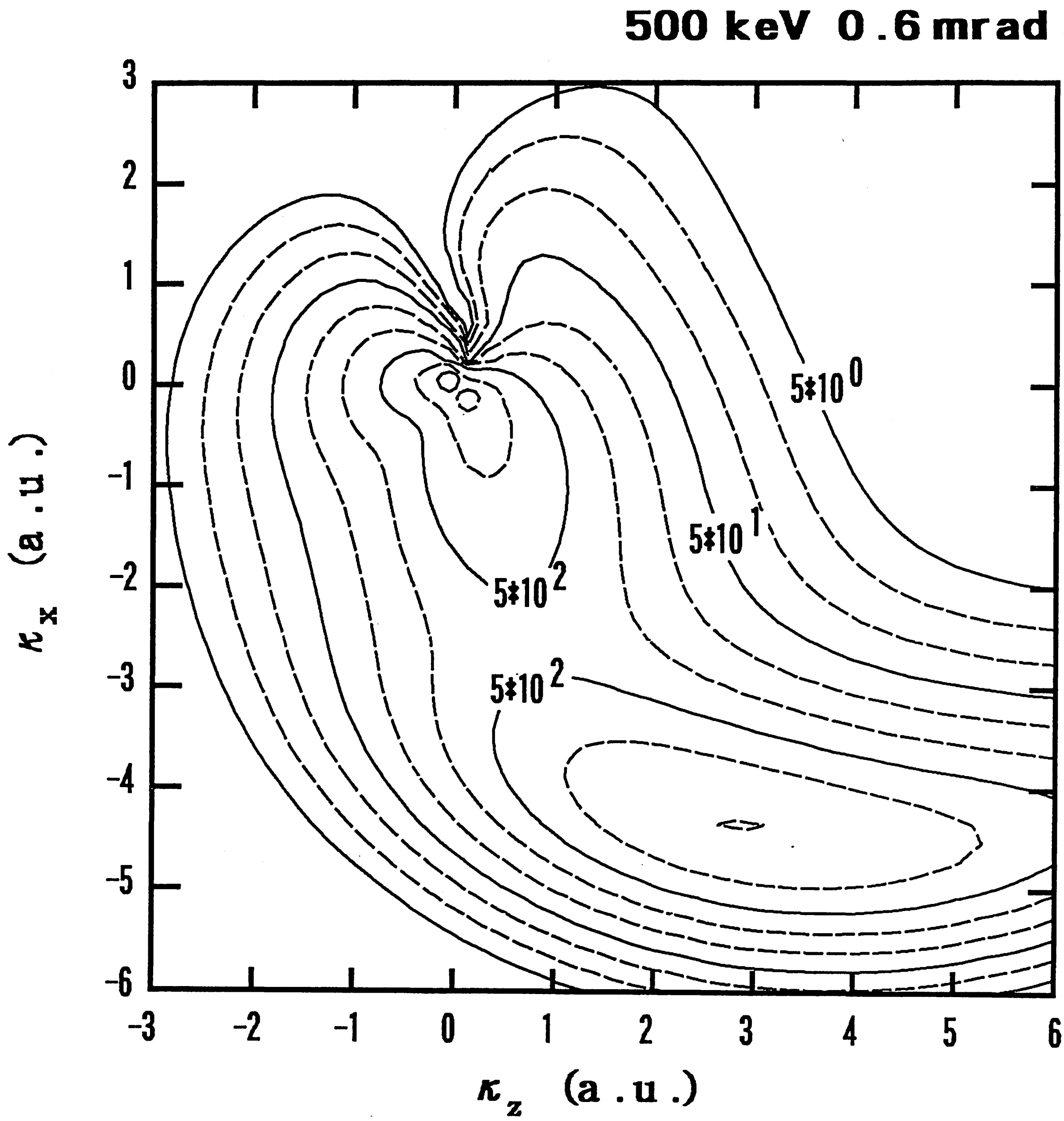

500 keV 0.6 mrad
5*10 0
5*10 1
5*10 2
5*10 2
3
2
1
0
-1
-2
-3
-4
-5
-6
-3
-2
-1
0
1
2
3
4
5
6
κx (a.u.)
κz (a.u.)

Fig. 1(c)

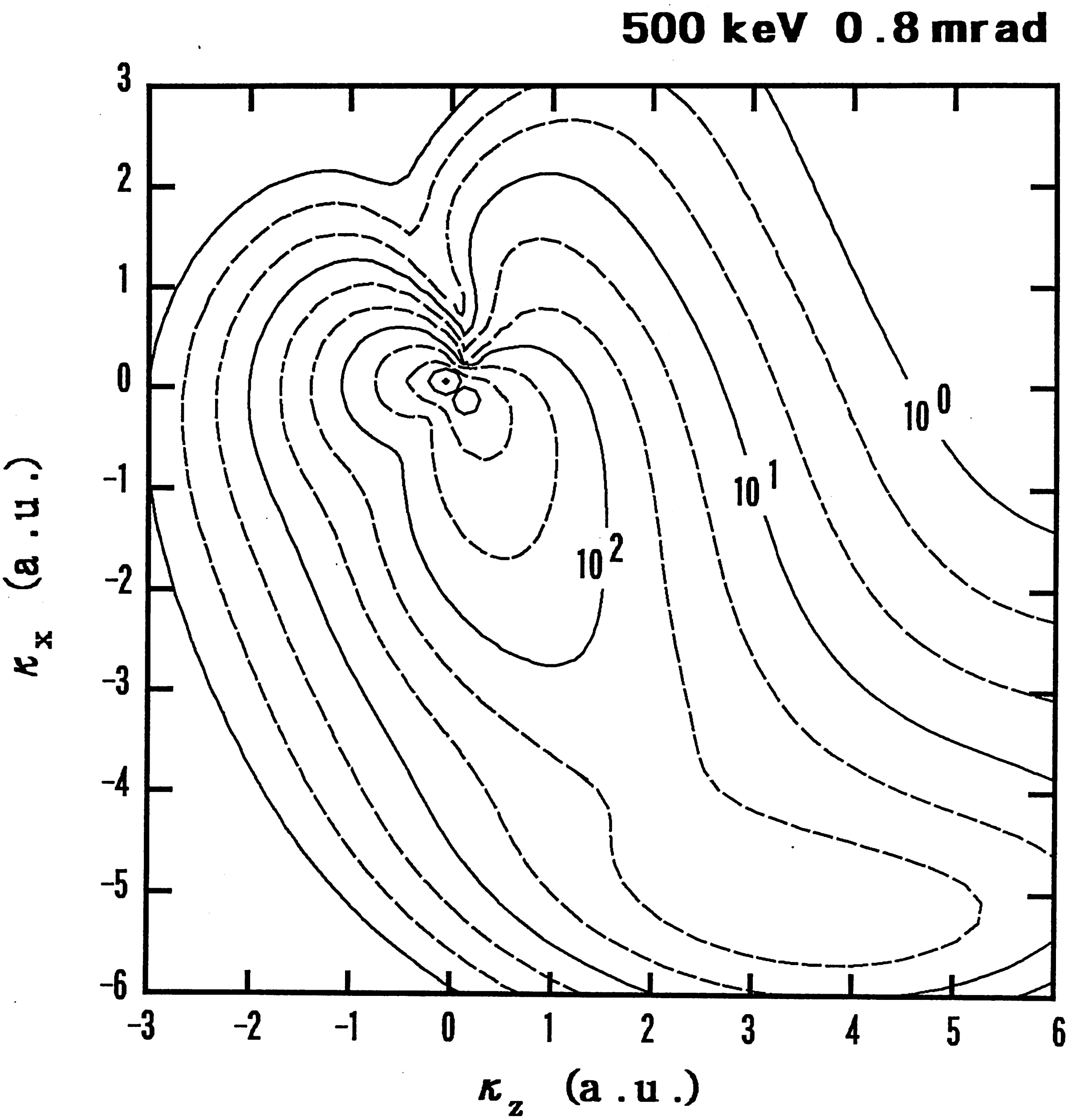

Fig. 1(d)

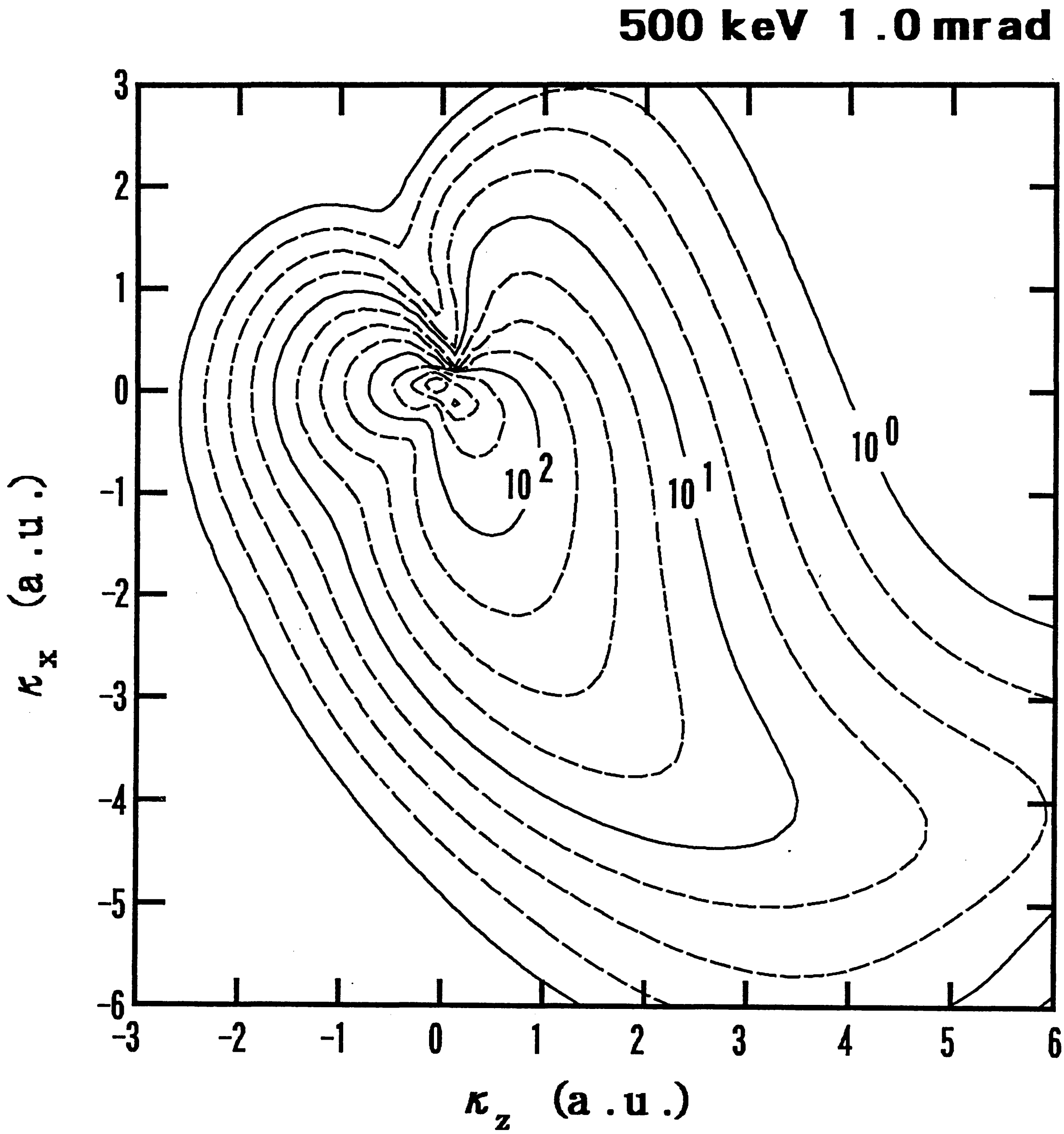
500 keV 1.0 mrad
3
2
1
0
-1
-2
-3
-4
-5
-6
-3
-2
-1
0
1
2
3
4
5
6
κ_x (a.u.)
κ_z (a.u.)
10^2
10^1
10^0

Fig. 1(e)

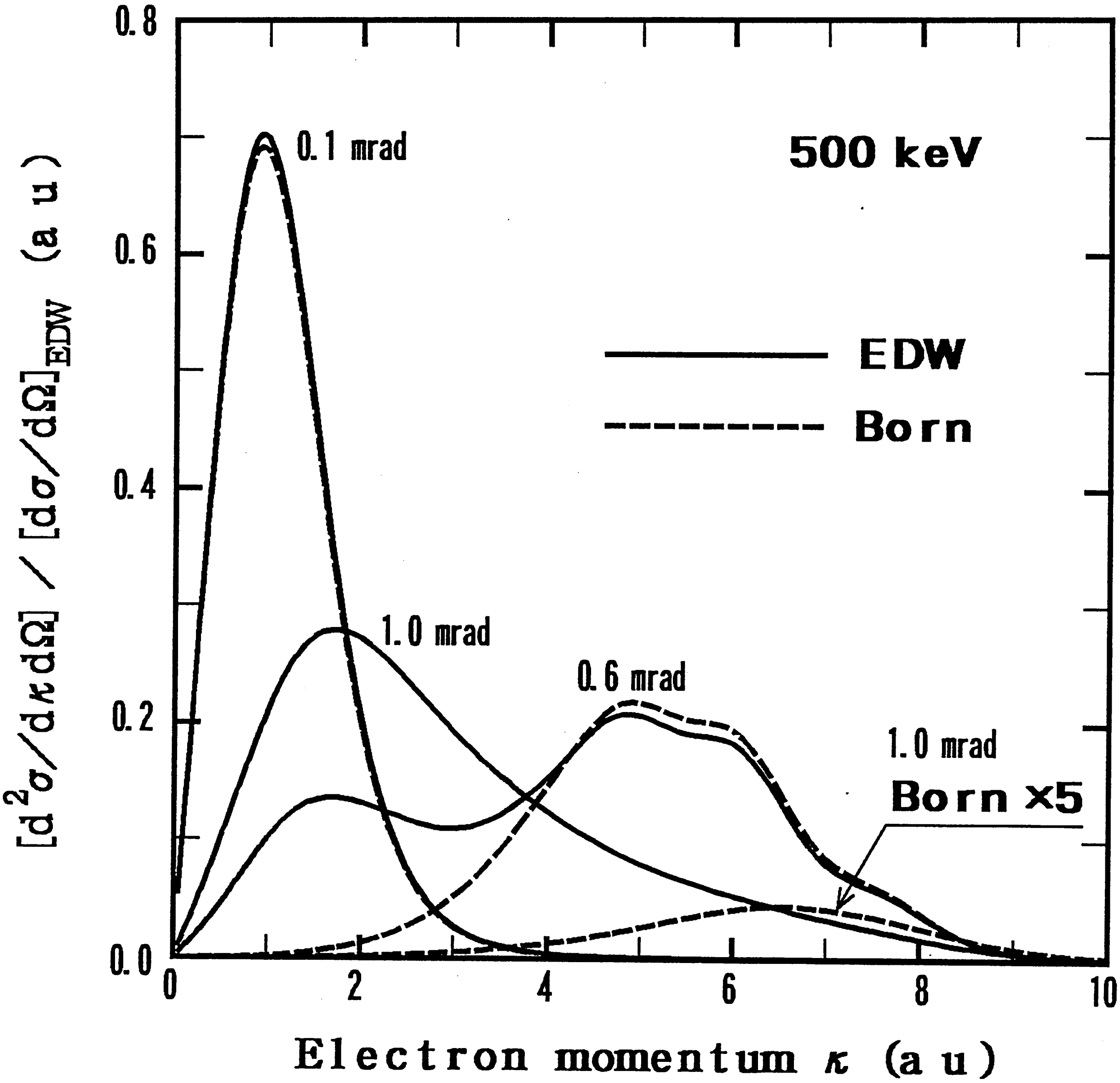

0.8
0.6
0.4
0.2
0.0
0
2
4
6
8
10
0.1 mrad
500 keV
EDW
Born
1.0 mrad
0.6 mrad
1.0 mrad
Born ×5
$[d^2\sigma/d\kappa d\Omega]$ / $[d\sigma/d\Omega]_{EDW}$ (a u)
Electron momentum κ (a u)

Fig. 2

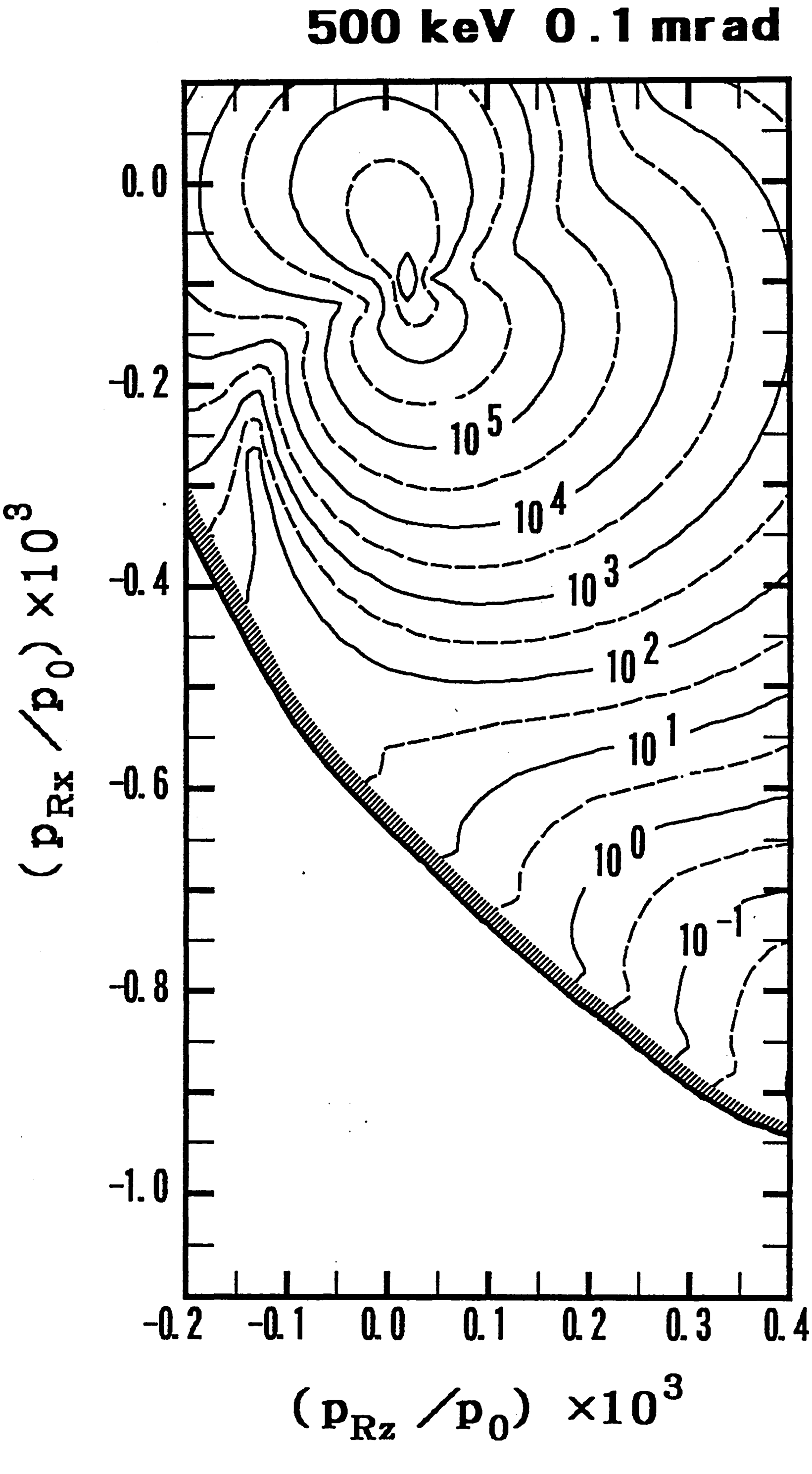

500 keV 0.1 mrad
0.0
-0.2
-0.4
-0.6
-0.8
-1.0
-0.2
-0.1
0.0
0.1
0.2
0.3
0.4
10^5
10^4
10^3
10^2
10^1
10^0
10^{-1}
$(p_{Rx}/p_0)\times10^3$
$(p_{Rz}/p_0)\times10^3$

Fig. 3(a)

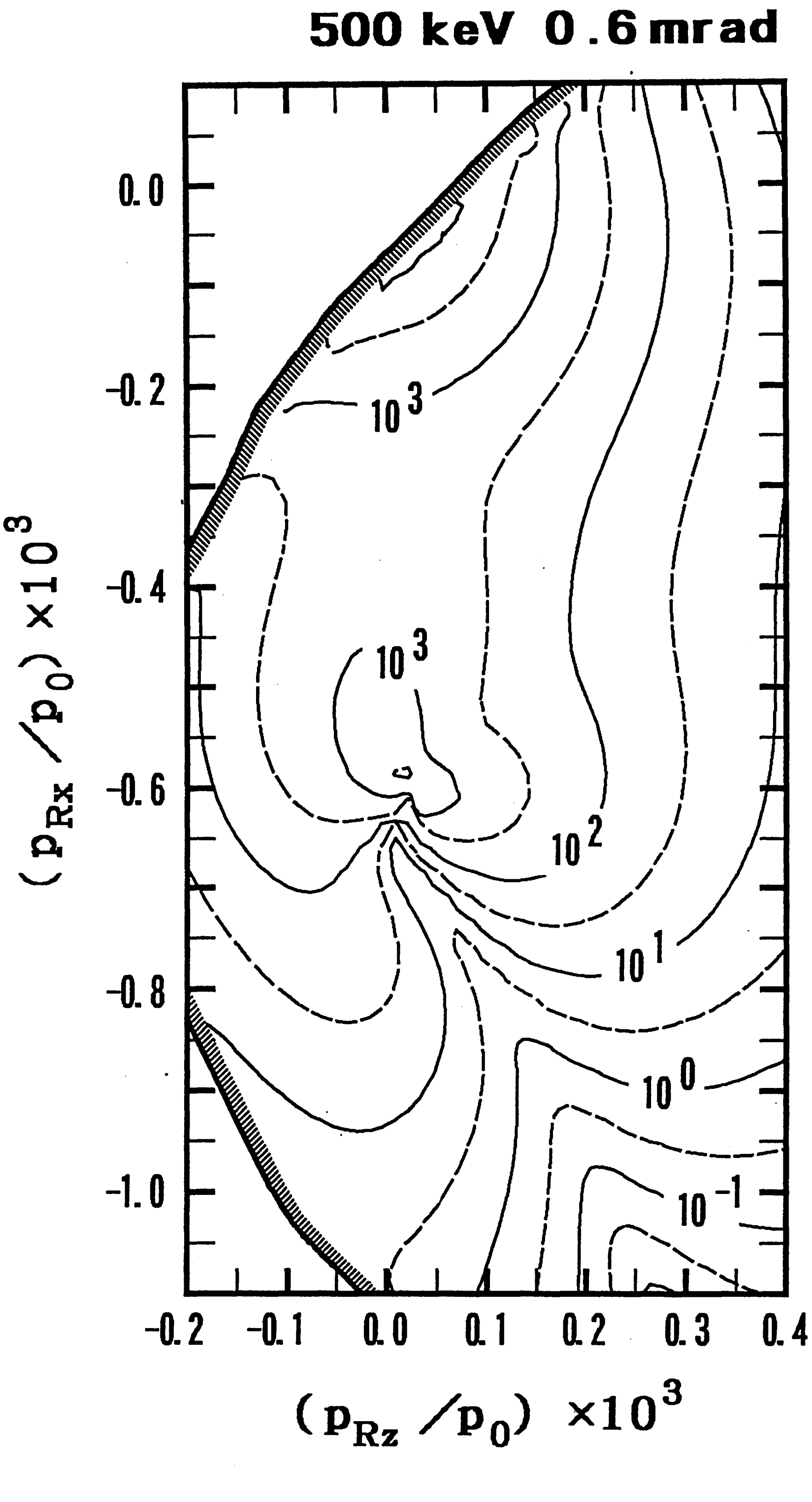

500 keV 0.6 mrad
0.0
-0.2
-0.4
-0.6
-0.8
-1.0
-0.2
-0.1
0.0
0.1
0.2
0.3
0.4
$(p_{Rx}/p_0) \times 10^3$
$(p_{Rz}/p_0) \times 10^3$
10^3
10^3
10^2
10^1
10^0
10^{-1}

Fig. 3(b)

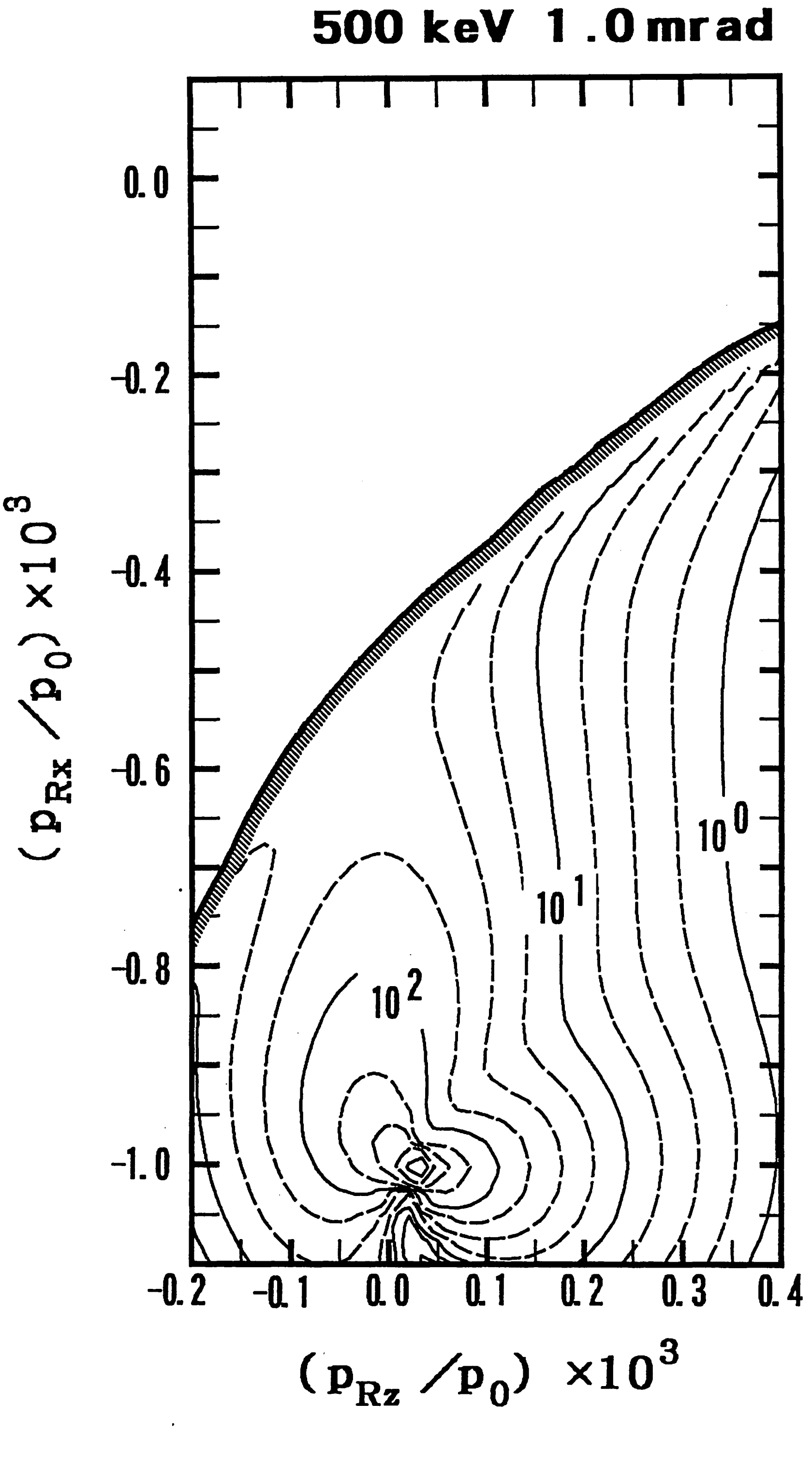

500 keV 1.0 mrad
0.0
-0.2
-0.4
-0.6
-0.8
-1.0
$(p_{Rx}/p_0)\times10^3$
10^0
10^1
10^2
-0.2
-0.1
0.0
0.1
0.2
0.3
0.4
$(p_{Rz}/p_0)\times10^3$

Fig. 3(c)

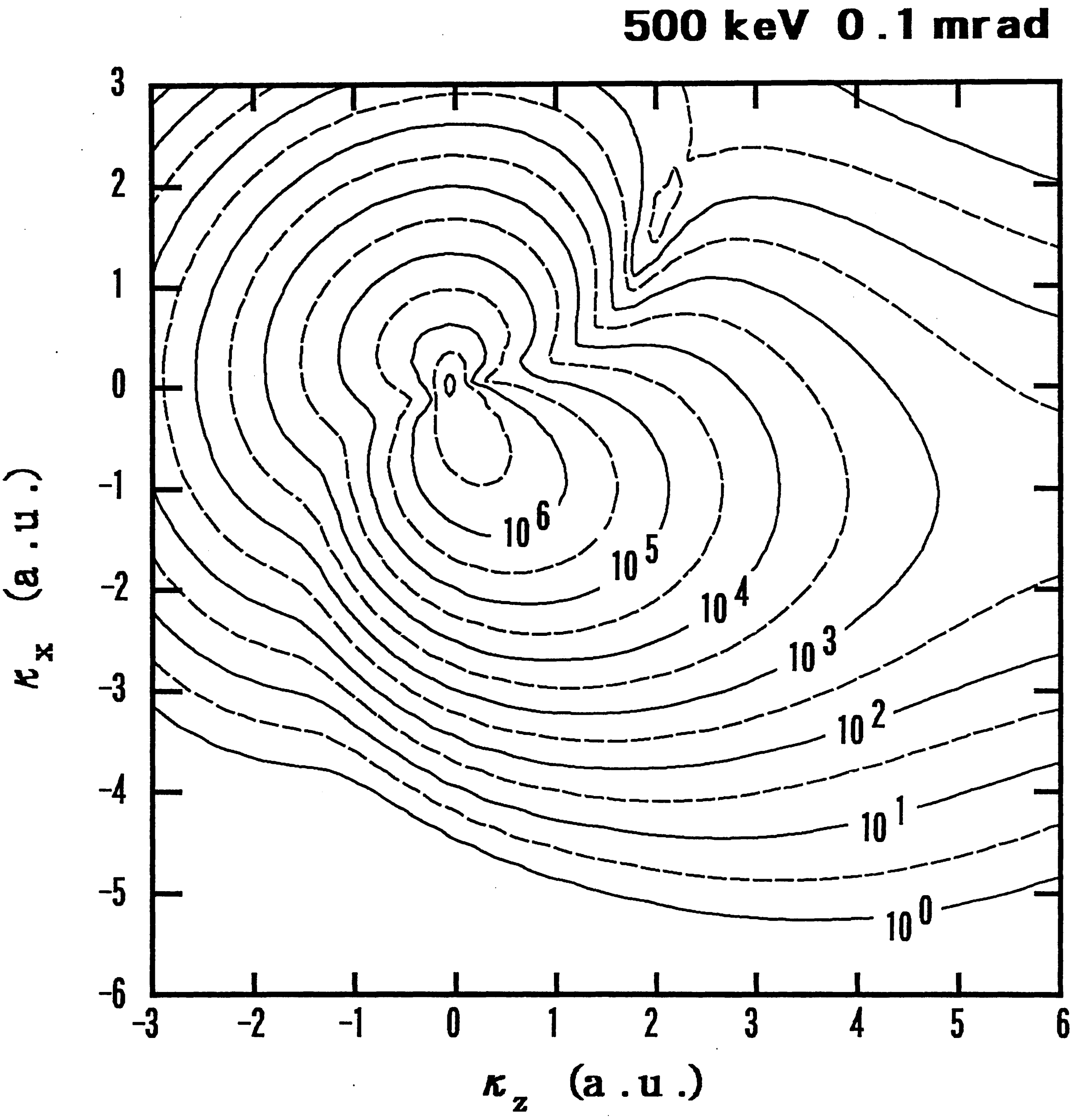

500 keV 0.1 mrad
κ_x (a.u.)
κ_z (a.u.)
10^6
10^5
10^4
10^3
10^2
10^1
10^0
3
2
1
0
-1
-2
-3
-4
-5
-6
-3
-2
-1
0
1
2
3
4
5
6

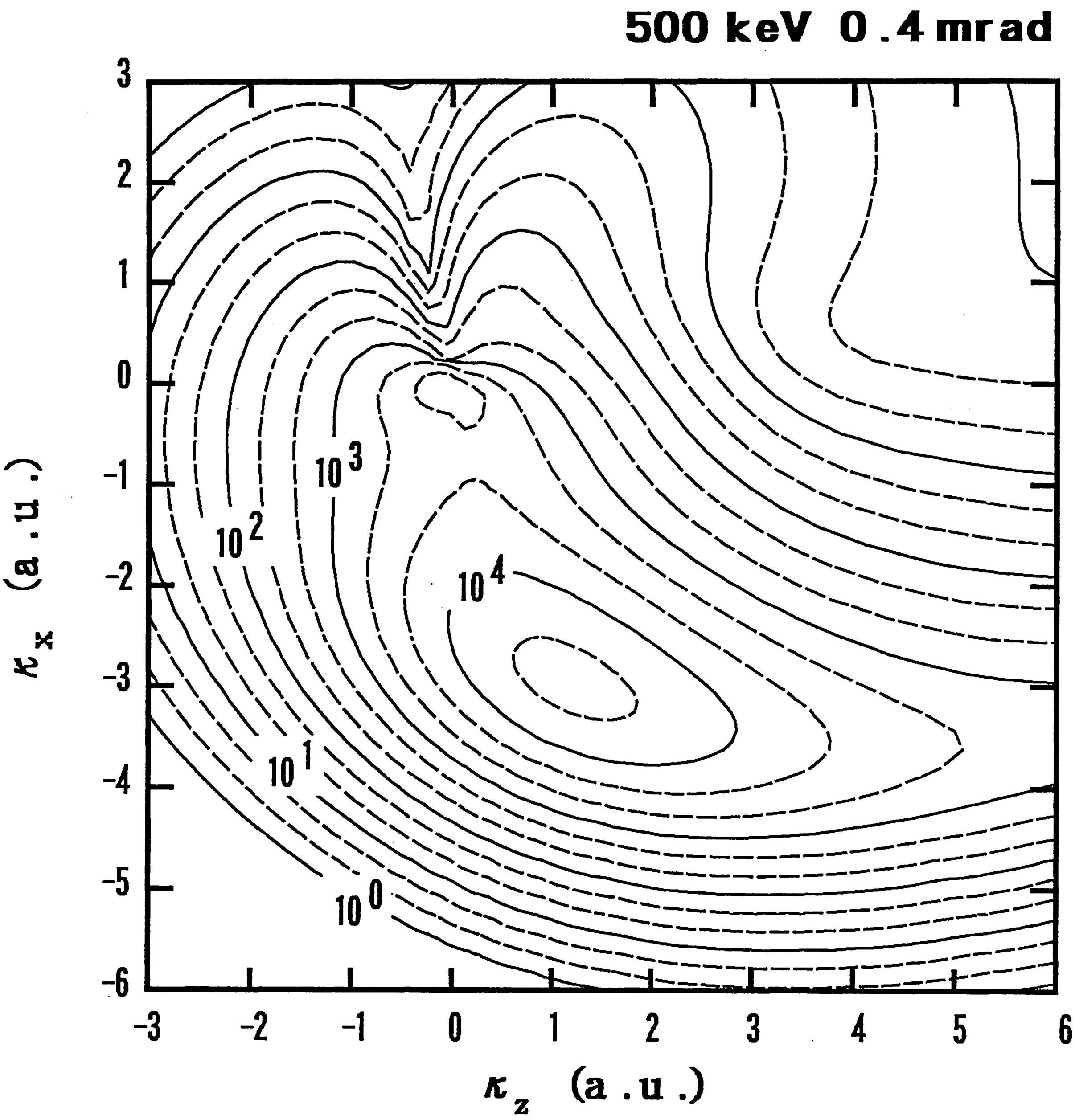
500 keV 0.4 mrad
3
2
1
0
-1
-2
-3
-4
-5
-6
-3
-2
-1
0
1
2
3
4
5
6
10 3
10 2
10 4
10 1
10 0
κ_x (a.u.)
κ_z (a.u.)

500 keV 0.6 mrad

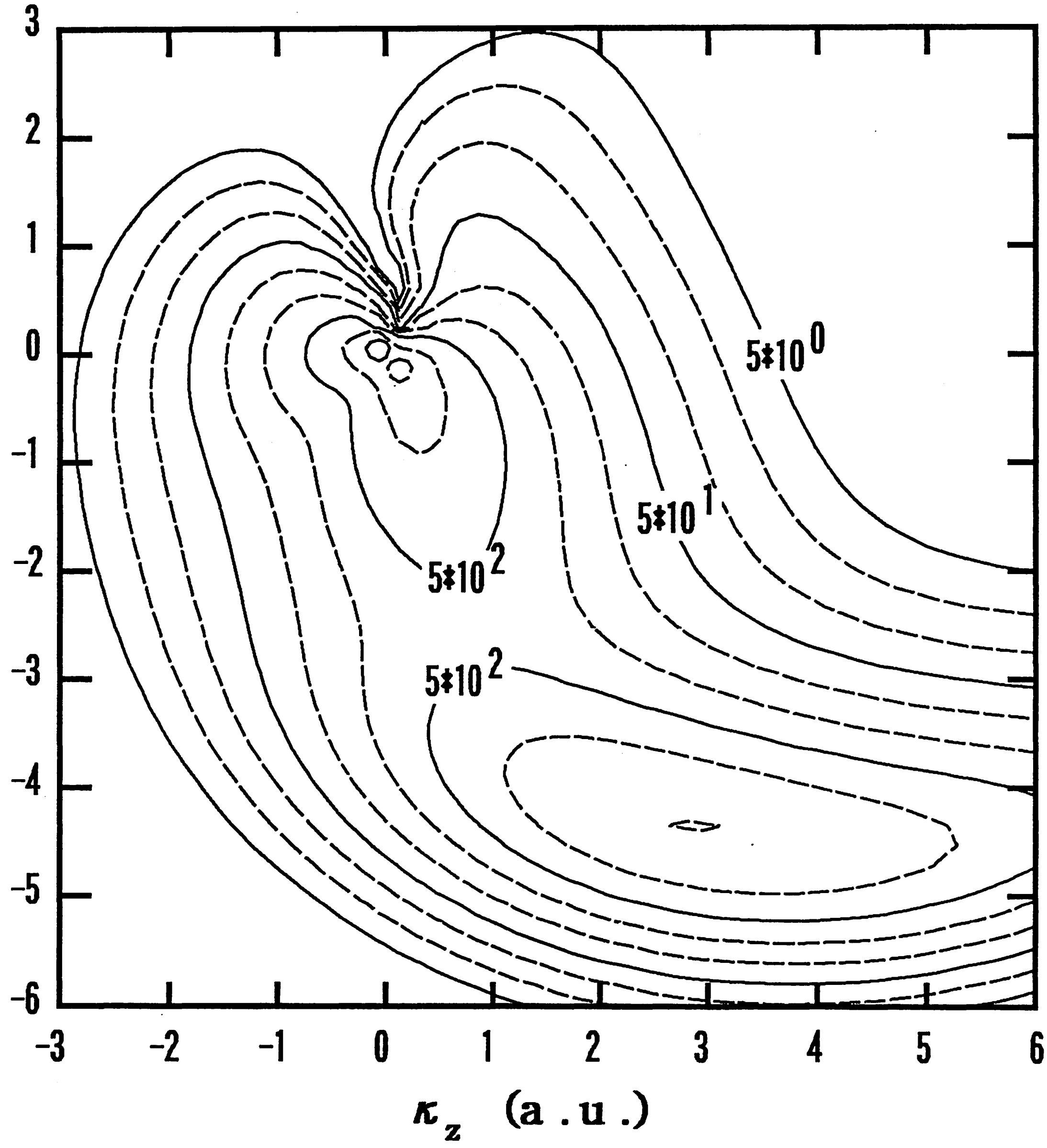

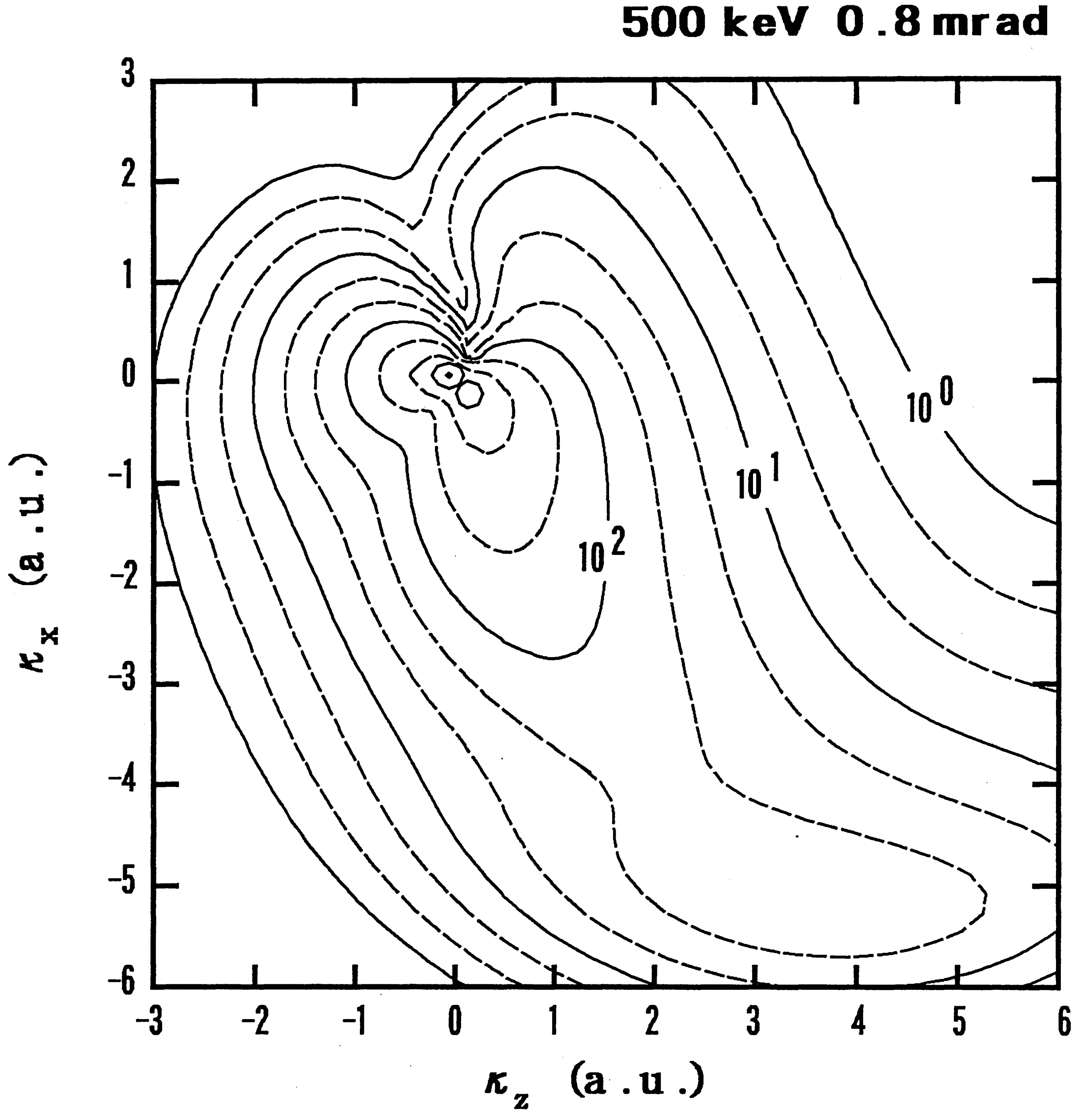

500 keV 0.8 mrad
3
2
1
0
-1
-2
-3
-4
-5
-6
κ_x (a.u.)
-3
-2
-1
0
1
2
3
4
5
6
κ_z (a.u.)
10^0
10^1
10^2

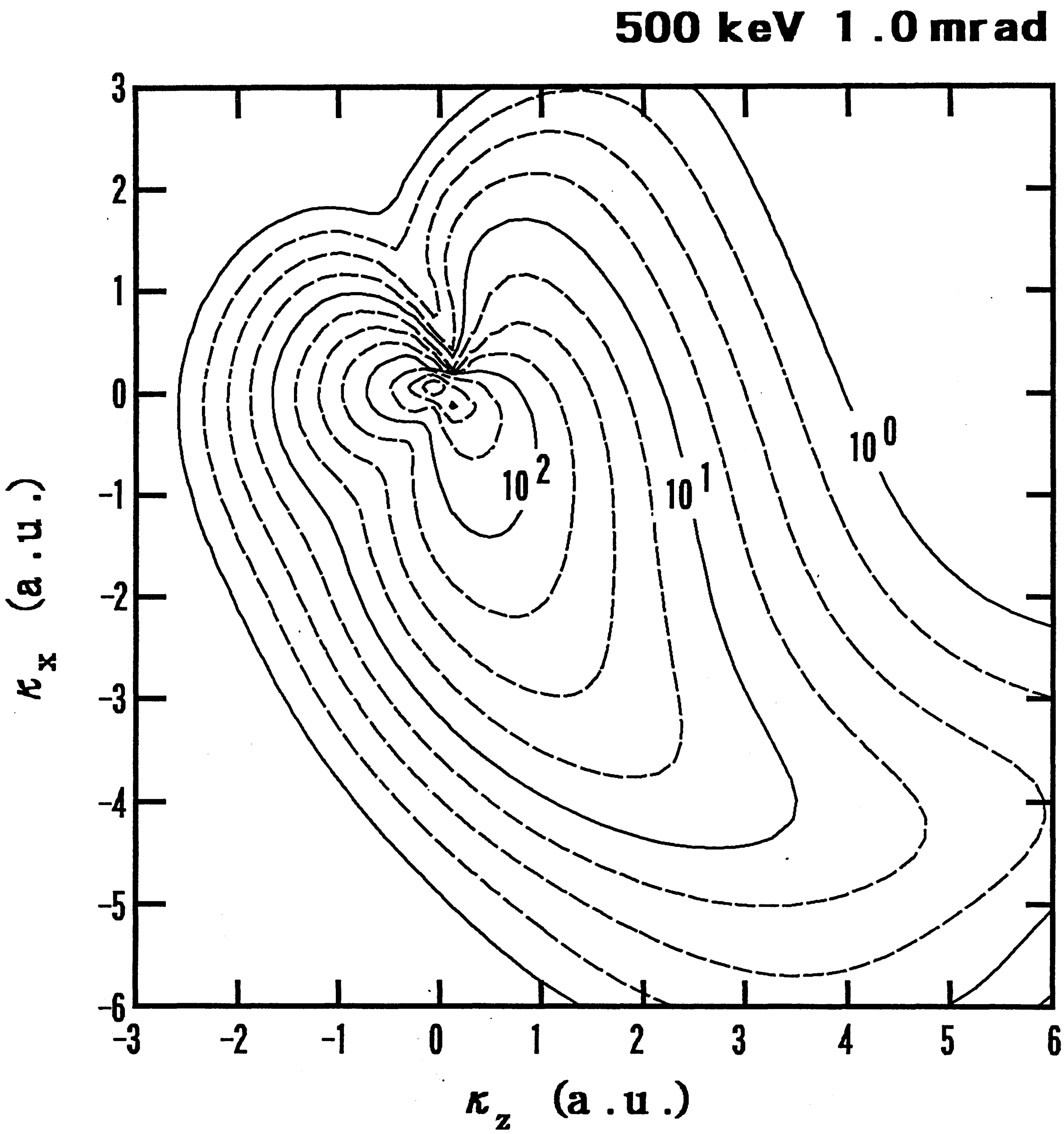

500 keV 1.0 mrad
10^2
10^1
10^0
κ_x (a.u.)
κ_z (a.u.)
3
2
1
0
-1
-2
-3
-4
-5
-6
-3
-2
-1
0
1
2
3
4
5
6

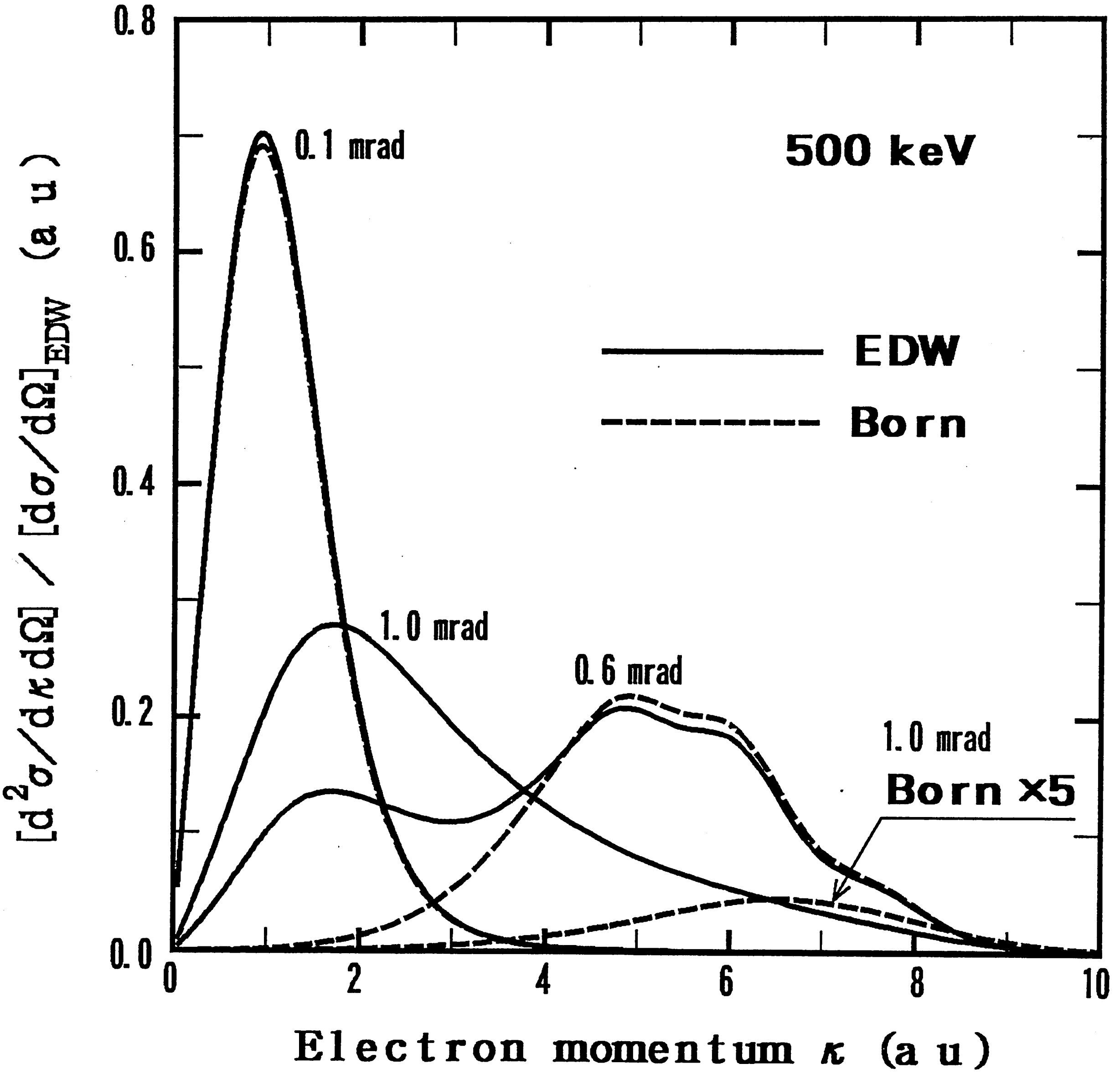

500 keV
EDW
Born
0.1 mrad
1.0 mrad
0.6 mrad
1.0 mrad
Born ×5
0.0
0.2
0.4
0.6
0.8
0
2
4
6
8
10
[d²σ/dκdΩ] / [dσ/dΩ]EDW (a u)
Electron momentum κ (a u)

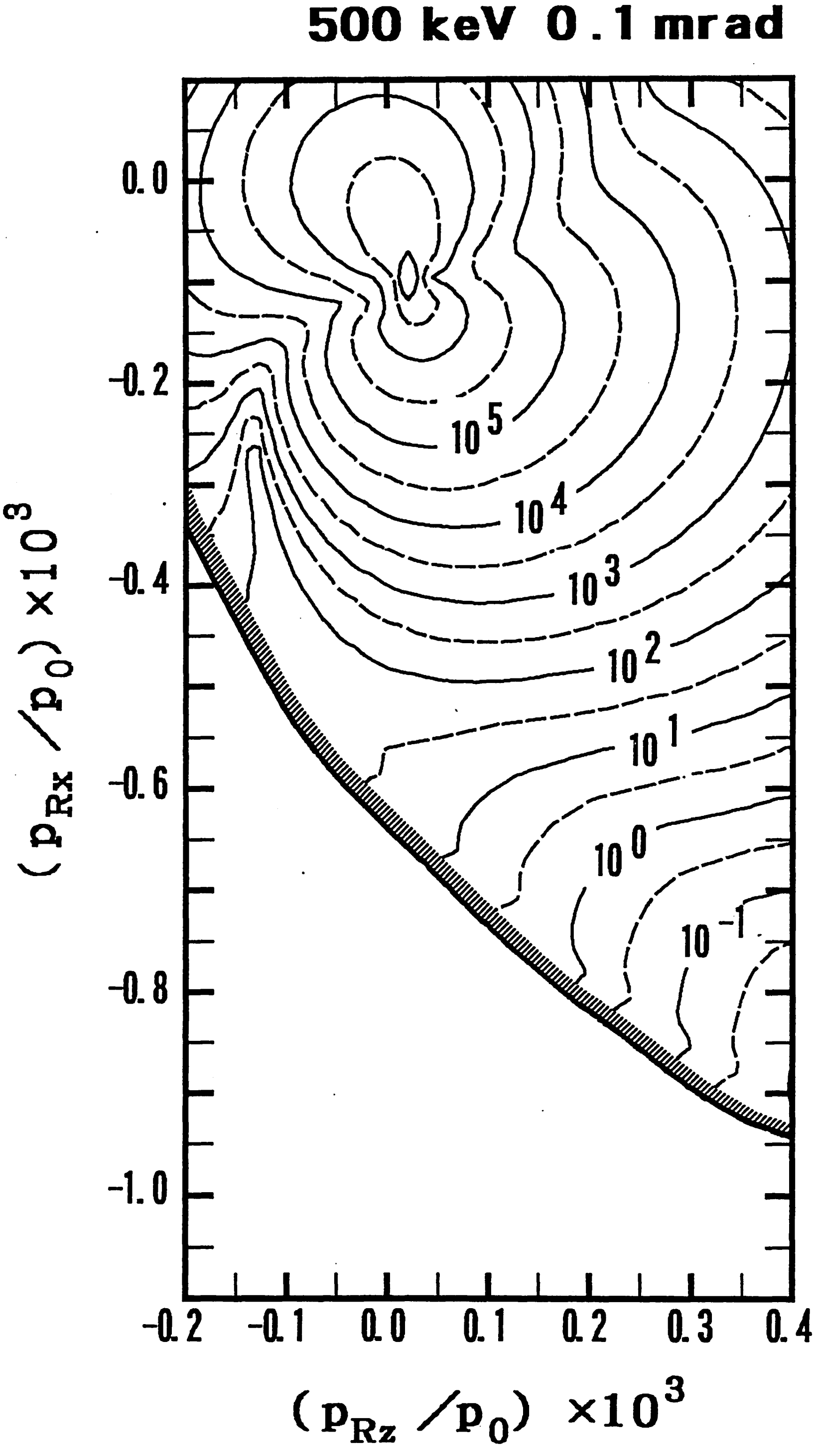

500 keV 0.1 mrad
10^5
10^4
10^3
10^2
10^1
10^0
10^-1
0.0
-0.2
-0.4
-0.6
-0.8
-1.0
-0.2
-0.1
0.0
0.1
0.2
0.3
0.4
(p_Rx / p_0) ×10^3
(p_Rz / p_0) ×10^3

500 keV 0.6 mrad

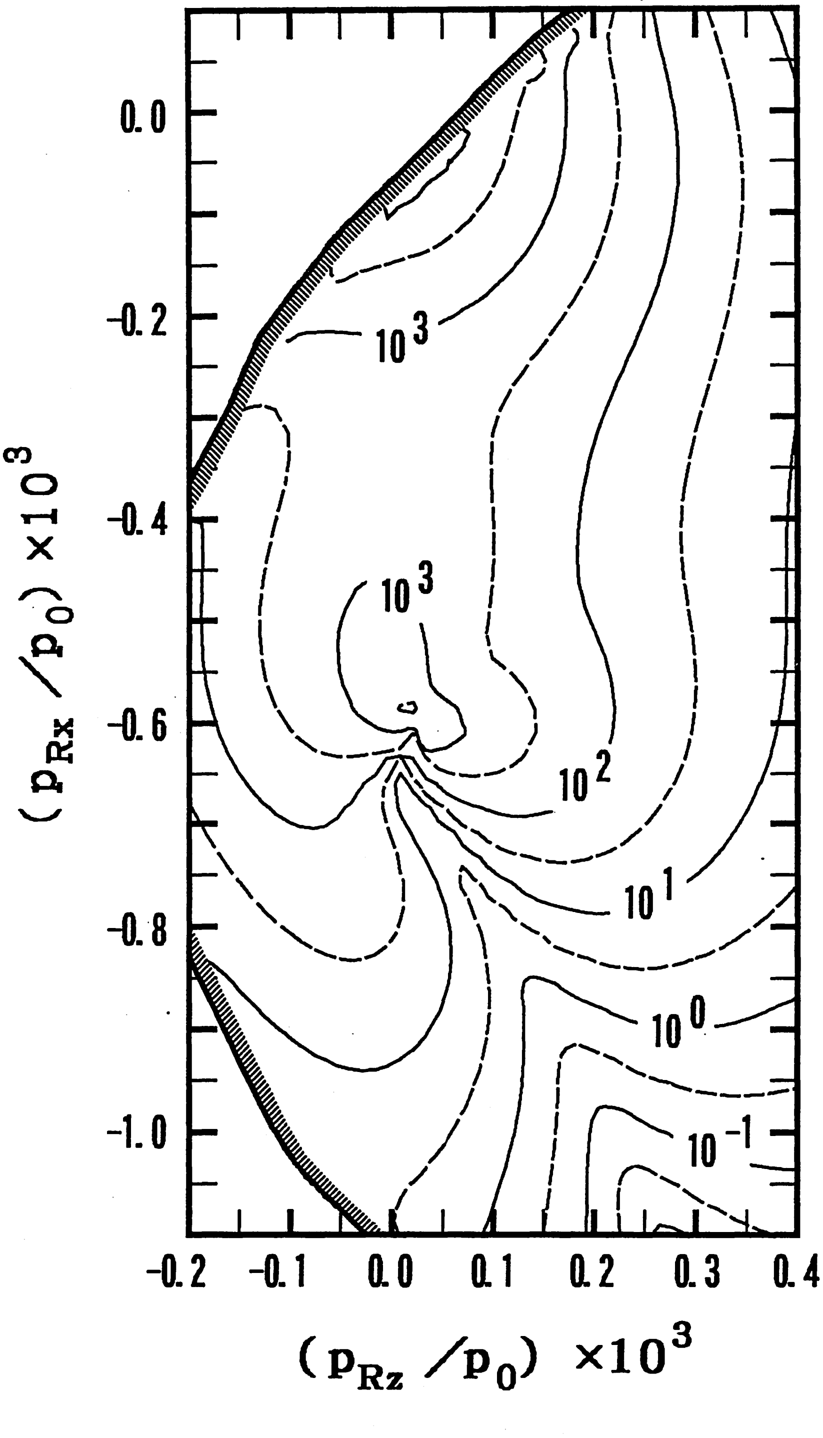

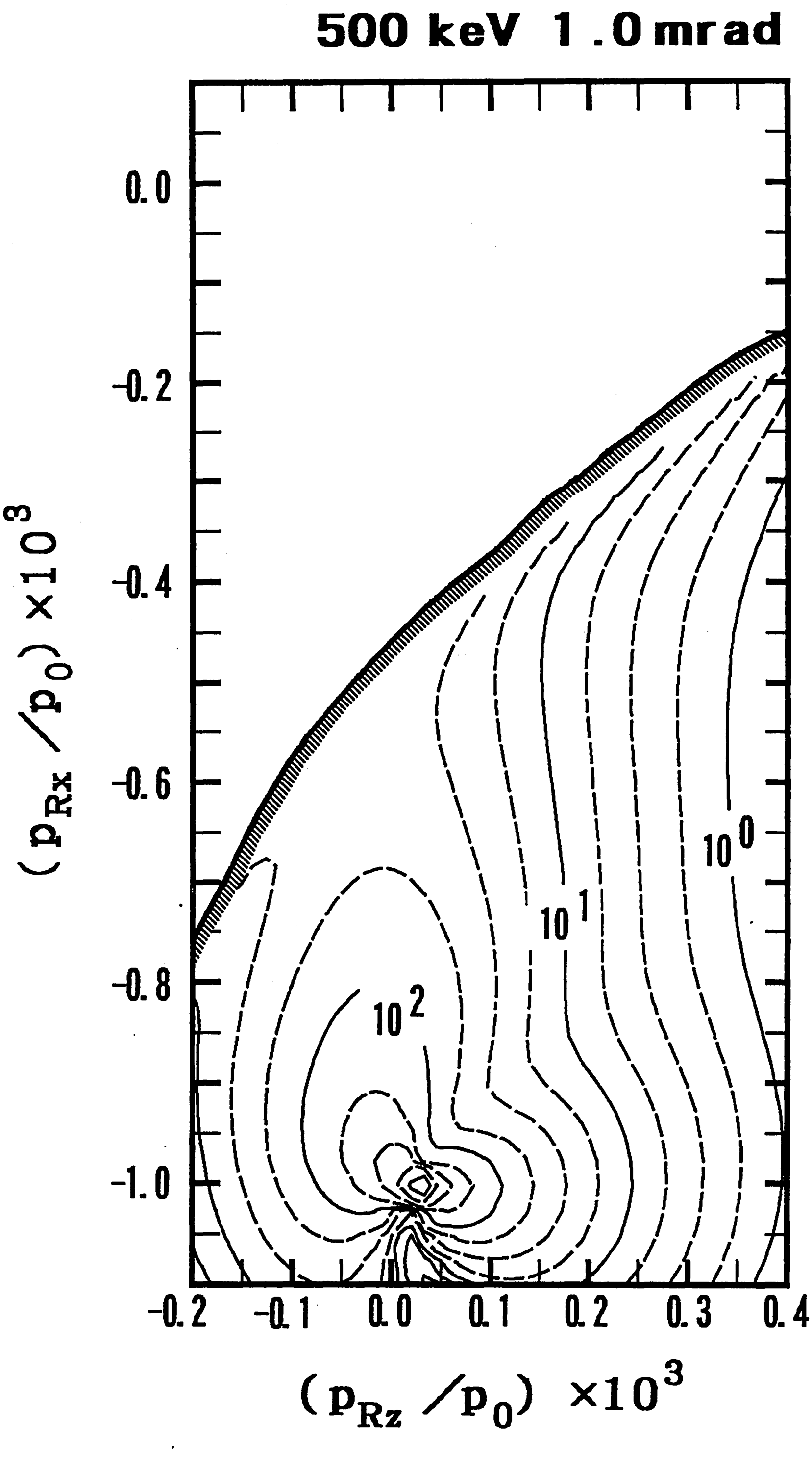

500 keV 1.0 mrad
0.0
-0.2
-0.4
-0.6
-0.8
-1.0
$(p_{Rx}/p_0)\times10^3$
-0.2
-0.1
0.0
0.1
0.2
0.3
0.4
$(p_{Rz}/p_0)\times10^3$
10^0
10^1
10^2